

Transportation of nanomaterial Maxwell fluid flow with chemical reaction under the second orderslips effect: Nonlinear stretching

M. N. Khan¹, Nadeem Abbas¹

¹Mathematics of Mathematics, Quaid-I-Azam University 45320, Islamabad 44000, Pakistan.

ABSTRACT

Nanomaterial Maxwell fluid flow under the second-grade slip effects over vertical nonlinear stretching sheet is considered in this analysis. The effects of Viscous dissipation and thermal slip at the exponential sheet are taken into account. Buongiorno's model effects on the Maxwell fluid are also taken into the present analysis. The PDE's are constructed after applying the boundary layer approximations after using the flow assumption. These PDE's further transformed into ODE's by means of the similarity transformations. The ODE's are solved to analyze the flow behavior through numerical scheme bvp4c. The impacts of the governing physical parameters are represented in the form of tables and graphs. Moreover, the comparison table is also added which found to be present results good agree with decay result. These results may be used in the field of industrial which proved to be more efficient. The velocity profile enhances due to enhancing the values of λ while the velocity profile declines as rises the values of δ . Velocity function decays, as well as the values of the β , rises, and the values of the $f'(\eta)$ enhances due to enhances the values of Nr .

Key words: Maxwell fluid; Viscous dissipation and Mixed convection; Buongiorno's model.

Date of Submission: 12-09-2022

Date of Acceptance: 28-09-2022

Nomenclature

u_w	stretching surface velocity (m/s)	D_T	thermophoretic diffusion coefficient (m^2/s)
u	velocity along x -direction (m/s)	D_B	Brownian diffusion coefficient (m^2/s)
v	velocity along y -direction (m/s)	D_{CT}	Soret diffusivity coefficient (m^2/s)
C	volume concentration	α_m	thermal diffusion coefficient (m^2/s)
C_w	wall concentration	k	thermal conductivity (W/mK)
C_∞	ambient concentration	SNu_x	Regular Nusselt number
T	Temperature (K)	Sh_x	Sherwood number
T_w	wall temperature (K)	Nu_x	Nusselt number
T_∞	ambient temperature (K)	Nb	Brownian motion parameter
Nt	Thermophoresis parameter	Re_x	local Reynolds number
Sc	Schmidt number ($Sc = v/D_B$)	Le	Lewis number ($Sc = \alpha/D_B$)
$f(\eta)$	dimensionless velocity factor	Pr	Prandtl number ($Pr = \nu/\alpha$)
$\theta(\eta)$	dimensionless temperature factor	M	Magnetic field parameter
u_0	dimensional constant ($1/s$)	Ec	Eckert number
$h(\eta)$	dimensionless nanoparticle factor	Bi	Biot number
Gr_x	Grashof number	B_0	external magnetic field
h_w	Heat transport coefficient	u_e	Free stream velocity (m/s)
q_w	surface mass flux ($kg/m^2 s$)	q_m	surface mass flux (W/m^2)
g	Gravity (m/s^2)	c_p	specific heat capacity (J/kgK)
D_T	Thermal diffusivity coefficient (m^2/s)	D_B	Mass diffusivity coefficient (m^2/s)
Nr	Regular buoyancy ratio parameter	D_s	Solutal diffusivity coefficient (m^2/s)
Nc	Buoyancy ratio parameter		

Greek Symbols

τ	Ratio of heat capacity to the base fluid	μ_e	magnetic permeability (N/A^2)
$\gamma(\eta)$	dimensionless concentration factor	σ	electrical conductivity (s/m)
λ	Mixed convection parameter	ρ_f	density of fluid (kg/m^3)
ψ	stream function (m^2/s)	η	similarity variable
μ	dynamic viscosity (kg/ms)	ν	kinematic viscosity (m^2/s)
λ_1	relaxation time of fluid	β	Deborah number ($\beta = \lambda(t)/t_{obs}$)
δ	Second order slip parameter	γ_1	First order slip parameter
β_C	volumetric solutal expansion coefficient ($1/mol$)	β_T	volumetric thermal expansion coefficient ($1/K$)

I. Introduction

The rheological characteristics of the fluid concerned play a crucial role in completing such activities successfully. In the past, various fluid models have been created to comprehend the rheological characteristics and mechanism of non-Newtonian fluid. Nonviscousfluid models of rate type and differential have achieved the researchers ' unique preference. A Maxwell fluid model is a rare type of fluid which predicts the impacts of relaxation time. This is a type of non-viscousfluid whichpredicts shear thinning of the fluid. Maxwell [1] was the first one who was poinreed the Maxwell fluid model. This idea much attracted from the several investigators because its several applications in the field of engineering processes and science. Sadeghy et al. [2] were highlighted the influence of upper convected of the Maxwell fluid over a moving plate. They predicted the results that Deborah number enhances with declining fraction factors. Mukhopadhyay et al. [3] were analyzed the properties of heat transfer of the Maxwell fluid model. They also debated the thermal radiation and unsteady parameter effects on a permeable sheet. They deliberated the results that Maxwell parameter and unsteadiness parameter enhances for rising the values of fraction factors. The uses of Maxwell fluid play a vital role in the field of fabulous in the polymer industry. This process basically involves transferring heat between the liquid and the surface covering it. Xu et al. [4] was pioneered the maxed convection of the Buongiorno mathematical model over vertical sheet. Nadeem et al. [5] have been highlighted the effects of Maxwell fluid flow over a stretching sheet.Khan et al. [6] analyzed the flow of siskonanofluid. Khan et al. [7] studied about the generalized Fourier's and Fick's laws based sisko fluid numerically. The effects of chemical reaction and activation energy in the Maxwell fluid at stretching sheet in the existence of rotating frame by Shafique et al. [8].Heat transfer of electrical MHD effects of Maxwell fluid has been discussed by Hsiao [9]. Hsiao [9] has also deliberated the inspiration of radiative and viscous dissipation. Aman et al. [10] inspected the flow of Oldroyd-B fluid numerically. Aman et al. [11] deliberated the Maxwell fluid flow over a sheet under the second order slip effects. There are many investigators are discussed the Maxwell fluid flow under different physical assumptions see in Refs. [12-18].

Convectional heat transfer of base fluid, namely Engine oil, Ethylene glycol, Water, have played a vital role in the field of thermal system. Heat transfer of these liquids is limited because low thermal characteristics which shows low performances. Suspending non-metallic and metallic solid particles in them is a creative way to develop the thermal properties of traditional fluids.These types of the fluids which suspended base fluid and nanomaterial is called Nanofluid. Choi and Eastman [19] were pioneered of nanofluid. This presentation made very high impressive. Although most solid particles have lower thermal conductivities than traditional heat transfer liquids, high heat transfer efficiency can be achieved when conventional liquids disperse these crystals. Lee et al. [20] worked on the time dependent fluid properties in the low volume friction. They performed experimentally and gained initiative results. Buongiorno [21] was pioneered the idea about the convective transformation of the nanofluid. He also highlighted the influence of Brownian diffusion. Due to buoyancy forces presences of partial heated rectangular, natural convection of nanomaterial fluid flow is presented by Oztop and Nada [22]. Santra et al. [23] presented the idea about numerical results of laminar nanofluid flow over two partially heated rectangle plate isothermally. Lots of interest gained by authers to analyzed the flow over stretching sheet. Nadeem et al. [24] deliberate the analysis of heat transfer of based micropolar fluid. The effects of micropolar fluid flow at Riga plate also considered in thier analysis. The impacts of based modified nanofluid flow also highlighted by Nadeem et al. [25].Alblawi et al. [26] discussed the nonlinear stretching sheet under Buongiorno's model of the fluid. Awan et al. [27] discussed the numerical solution of the anti-cubic nonlinearity. Ozair et al. [28] investigated the Bio-inspired analytical results of heuristics. Awan et al. [29] investigated the Jeffrey nanofluid at stretching sheet. Recently, numerous investigators are discussed the flos behavior under the different assumptions see in Refs. [30-35].

Nanomaterial Maxwell fluid flow under the second grade slip effects over vertical nonlinear stretching sheet is considered in this analysis. The effects of Viscous dissipation and thermal slip at the exponentially sheet is taken into account. The PDE's are constructed after applying the boundary layer approximations after using the flow assumption. These PDE's further transformed into ODE's by means of the similarity transformations. The ODE's are solved to analyze the flow behavior through numerical scheme bvp4c. The impacts of the governing physical parameters are represented in the form of tables and graphs.More over, the comparision table is also added which found to be present results good agree with decay result. No one higligjhted thee effects of Maxwell nanomaterial fluid flow at a stretching sheet with second grade slip effects. These results may used in the field of industrial which proved to be more efficient.

II. Flow analysis

The flow analysis of maxwellnanofluidata vertical stretching surface is deliberated. The chemical reactions and second grade slip effects are also deliberated in the current study. The system of differential equations is constructed through the boundary layer approximation on the mathematical model using the Navior stock equations. The following equations are as bellow (see Refs. [11, 36])

$$\frac{\partial u}{\partial x} + \frac{\partial v}{\partial y} = 0, \quad 1$$

$$u \frac{\partial u}{\partial x} + v \frac{\partial u}{\partial y} + \lambda_1 \left(u^2 \frac{\partial^2 u}{\partial x^2} + v^2 \frac{\partial^2 u}{\partial y^2} + 2uv \frac{\partial^2 u}{\partial x \partial y} \right) = \begin{pmatrix} \nu \left(\frac{\partial^2 u}{\partial y^2} \right) + u_e \frac{du_e}{dx} + \frac{\sigma B_0^2}{\rho_f} (u_e - u) \\ +(1 - \phi_\infty) g [\beta_T (T - T_\infty) - \beta_C (C - C_\infty)] \\ + g \left(\frac{\rho_f - \rho_p}{\rho_f} \right) (\phi - \phi_\infty) \end{pmatrix} \quad 2$$

$$u \frac{\partial T}{\partial x} + v \frac{\partial T}{\partial y} = \alpha_m \frac{\partial^2 T}{\partial y^2} + \tau D_B \frac{\partial T}{\partial y} \frac{\partial \phi}{\partial y} + \frac{\tau D_T}{T_\infty} \left(\frac{\partial T}{\partial y} \right)^2 + \frac{\nu}{\rho_f c_p} \left(\frac{\partial u}{\partial y} \right)^2 \quad 3$$

$$u \frac{\partial \phi}{\partial x} + v \frac{\partial \phi}{\partial y} = D_B \left(\frac{\partial^2 \phi}{\partial y^2} \right) + \frac{D_T}{T_\infty} \frac{\partial^2 T}{\partial y^2} \quad 4$$

$$u \frac{\partial C}{\partial x} + v \frac{\partial C}{\partial y} = D_S \left(\frac{\partial^2 C}{\partial y^2} \right) + D_{CT} \frac{\partial^2 T}{\partial y^2} \quad 5$$

The related boundary conditions

$$\begin{aligned} u &= u_w + U_{slip} = u_w + A \frac{\partial u}{\partial y} + B \frac{\partial^2 u}{\partial y^2}, \quad v = 0 \\ -k \frac{\partial T}{\partial z} &= h_w (T_w - T), \quad \phi = \phi_w, \quad C = C_w. \text{ at } y \rightarrow 0 \\ u &= u_\infty, \quad T \rightarrow T_\infty, \phi = \phi_\infty, C \rightarrow C_\infty. \text{ at } y \rightarrow \infty \end{aligned} \quad 6$$

The velocity component in x - and y - directions are u and v respectively. The ρ_f is represents density of the fluid, ρ_p is the density of nanoparticles, fluid relaxation time is λ_1 , dynamic viscosity is ν , A and B are first and second order velocity slip factor, and c_p is the specific heat. D_T , D_B , D_S , and D_{CT} denotes the thermophoretic, Brownian, solutal diffusivity, and Soret diffusivity coefficient respectively. The h_w , σ , β_T , β_C , and g illustrates the heat transport coefficient, electrically conducting coefficient, volumetric thermal expansion coefficient, volumetric solutal expansion coefficient, and gravitational acceleration correspondingly. To transfer the above equations (1) – (6) into nonlinear ordinary differential equations we introduced following non dimensional variable [52],

$$\begin{aligned} \eta &= \sqrt{\frac{u_0}{2vl}} y \text{Exp} \left(\frac{x}{2l} \right), \quad u = u_0 \text{Exp} \left(\frac{x}{l} \right) f'(\eta), \quad \theta(\eta) = \frac{T - T_\infty}{T_w - T_\infty}, \quad h(\eta) = \frac{\phi - \phi_\infty}{\phi_w - \phi_\infty}, \\ v &= -\sqrt{\frac{vu_0}{2l}} \text{Exp} \left(\frac{x}{2l} \right) (f(\eta) + \eta f'(\eta)), \quad \gamma(\eta) = \frac{C - C_\infty}{C_w - C_\infty}, \end{aligned} \quad 7$$

Here T_0 , C_0 , and n_0 all are the constants. Using equation (8), the equation of continuity automatically holds and other equations in the form,

$$f''' + ff'' + 2\lambda(\theta + Nc\gamma - Nrh) + M(1 - f') + 1 - \beta(4f'^3 - \eta f'^2 f'' - 6ff' f'' + f''' f^2) = 0 \quad 8$$

$$\theta'' + Pr(f\theta' + Ec f'^2 + Nb\theta' h' + Nt\theta'^2) = 0 \quad 9$$

$$h'' + Lefh' + \frac{Nt}{Nb}\theta'' = 0 \quad 10$$

$$\gamma'' + Scf\gamma' + ScS_T\theta'' = 0 \quad 11$$

and

$$\begin{aligned} f(\eta) &= 0, \quad f'(\eta) = 1 + \gamma_1 f''(\eta) + \delta f'''(\eta) \\ \theta'(\eta) + Bi(1 - \theta(\eta)) &= 0, \quad h(\eta) = 1, \gamma(\eta) = 1 \text{ at } \eta \rightarrow 0, \\ f'(\eta) &= 1, \theta(\eta) = 0, h(\eta) = 0, \gamma(\eta) = 0. \text{ at } \eta \rightarrow \infty. \end{aligned} \quad 12$$

Here, prime denotes the derivative with respect to η . The Nr , Nc , β , M , λ , Nt , Nb , γ_1 , and δ are signifying the nanofluid buoyancy ratio, regular buoyancy, relaxation, magnetic field, mixed convection, thermophoresis, Brownian motion, first order slip, and second order slip parameters respectively. Further, r_x , Pr , Sc , Ec , S_T , Le , and Bi are represents the Grashof , Prandtl, Schmidt, Eckert, Soret, and Biot numbers respectively. The parameters are specified as,

$$\begin{aligned} \lambda &= \frac{Gr_x}{Re_x^2}, \quad \beta = \frac{\lambda_1 u_0}{2l}, \quad Pr = \frac{\nu}{\alpha_m}, \quad Le = \frac{\nu}{D_B}, \quad S_T = \frac{\Delta T D_{CT}}{\nu \Delta C}, \quad Bi = -\frac{h_w}{k} \sqrt{\frac{2vl}{u_0}}, \quad Sc = \frac{\nu}{D_S}, \\ M &= \frac{\sigma l B_0^2}{\rho u_w}, \quad \gamma_1 = A \sqrt{\frac{u_0}{2vl}}, \quad \delta = B \sqrt{\frac{u_0}{2vl}}, \quad Ec = \frac{u_w^2}{\Delta T c_p}, \quad Nt = \frac{\tau \Delta T D_T}{\nu T_\infty}, \quad Nb = \frac{\tau \Delta C D_B}{\nu}, \\ Nr &= \frac{(\phi_w - \phi_\infty)(\rho_f - \rho_p)}{\rho_f \beta_T (T_w - T_\infty)(1 - \phi_\infty)}, \quad Nc = \frac{\beta_C (T_w - T_\infty)}{\beta_T (T_w - T_\infty)}, \quad Gr_x = \frac{g \beta_T (T_w - T_\infty)(1 - \phi_\infty)}{\nu^2} x^3. \end{aligned} \quad 13$$

III. Physical quantities

From an engineering perspective the physical quantities such as local Nusselt, Sherwood, and microorganism numbers are most significant. These physical quantities observed the heat, mass, and microorganism transfer rate. These quantities are defined as,

$$Nu_x = \frac{xq_w}{k(T)(T_w - T_\infty)}, \quad NSh_x = \frac{xq_n}{D_B(\phi_w - \phi_\infty)}, \quad Sh_x = \frac{xq_m}{D_S(C_w - C_\infty)}. \quad 14$$

In equation (14) q_w , q_m , and q_n shows the heat, nanoparticles, and regular mass flux respectively, and they are delimited as,

$$q_w = -k \left(\frac{\partial T}{\partial y} \right) \Big|_{y=0}, \quad q_m = -D_B \left(\frac{\partial \phi}{\partial y} \right) \Big|_{y=0}, \quad q_n = -D_S \left(\frac{\partial C}{\partial y} \right) \Big|_{y=0}. \quad 15$$

In the dimensionless form,

$$Nu_x(Re_x)^{-\frac{1}{2}} = -\theta'(0), \quad NSh_x(Re_x)^{-\frac{1}{2}} = -h'(0), \quad Sh_x(Re_x)^{-\frac{1}{2}} = -\gamma'(0), \quad 16$$

The local Reynolds number is $Re_x = u_w \sqrt{\frac{2lu_0}{\nu}}$.

IV. Solution procedure

The system of equations (9) – (13) with equation (14) are solved numerically. To use a numerical method first we transfer the equations (9) – (14) into the first order differential equations. The solution of these equations adopted by means of bvp4c solution technique. The convergence criteria were assigned. The system of equations of first order:

$$\begin{pmatrix} f \\ f' \\ f'' \\ \theta \\ \theta' \\ h \\ h' \\ \gamma \\ \gamma' \end{pmatrix} = \begin{pmatrix} y(1) \\ y(2) \\ y(3) \\ y(4) \\ y(5) \\ y(6) \\ y(7) \\ y(8) \\ y(9) \end{pmatrix} \quad 17$$

$$f''' = yy_1 = \left[(1 - \beta y(1)^2)^{-1} (\beta \{4y(2)^3 - \eta y(2)^2 y(3) - 6y(1)y(2)y(3) + y(3)y(1)^2\}) - My(1)y(3) - 2\lambda(y(3) + Ncy(8) - Nry(6)) - 1 \right] \quad 18$$

$$\theta'' = yy_2 = Pr(-y(1)y(5) - Nby(5)y(7) - Nty(5)y(5) - Ecy(3)y(3)) \quad 19$$

$$h'' = yy_3 = -Ley(1)y(7) - \frac{Nt}{Nb} yy_2 \quad 20$$

$$\gamma'' = yy_4 = -Scy(1)y(9) - ScS_T yy_2. \quad 21$$

With boundary conditions are

$$y_0(1) = 0, y_0(2) = 1 + \gamma_1 y_0(3) + \delta yy_1, y_0(5) = -Bi(1 - y_0(4)), y_0(7) = 1, y_0(8) = 1, \quad 22$$

$$y_{inf}(2) = 1, y_{inf}(4) = y_{inf}(6) = y_{inf}(8) = 0.$$

V. Graphical results

Fig. 1 presents the inspirations of λ on the $f'(\eta)$. It is noted that the $f'(\eta)$ enhances for larger values of λ . The λ rises as the boundary layer thickness for away from the surface. Fig. 2 debates the inspiration of δ on the $f'(\eta)$. The curved of the $f'(\eta)$ presented the behavior decline towards surface as δ increases. Fig. 3 reveals the effects of γ_1 on the $f'(\eta)$. The $f'(\eta)$ reveals the curves away from the surface due to rise the values of γ_1 . The thickness of $f(\eta)$ away from the surface due to γ_1 rises. Fig. 4 exposes the impacts of M on the $f'(\eta)$. The velocity profile reveals decline curved near the surface when the values of M enhances. Fig. 5 reveals the impacts of β on the velocity profile. It is seen that velocity profile shows the declines curvcd due to β enhances. Variation of the Nr and $f'(\eta)$ which presented in Fig. 6. The curves of velocity show to be enhanced as Nr rises. The thickness of $f'(\eta)$ away from the surface, when the values of Nr enhances. Fig. 7 exposes the inspiration of Nc on $f'(\eta)$. It is noticed that curved of the velocity profile for away from the surface, the values of Nc enhances. Fig. 8 depicts the inspiration of Bi on the $\theta(\eta)$. The values of Bi increases which shows to enhancing the curved of $\theta(\eta)$. Fig. 9 depicts the effects of Ec on the temperatur profile. It is precied that $\theta(\eta)$ spectacles the curved enhances near the thermal boundary layer thickness when the values of Ec enhances. Fig. 10 depicts the influences of Pr on the $\theta(\eta)$. It is noted that curved of $\theta(\eta)$ found to be decreasing as Pr rises. Fig. 11 depicts the influence of Sc on $\gamma(\eta)$. The $\gamma(\eta)$ reveals the decline curves for higher values of Sc nea the surface. Fig. 12 debates the inspiration of S_T on $\gamma(\eta)$. The the values of S_T and $\gamma(\eta)$ found to be same behavior of increasing near the surface. Figs. 13-14 depict the influence of Le and Nb on the $h(\eta)$. The curved of $h(\eta)$

increasing for the higher values of Le and declines behavior for Nb rises. Fig. 15 exposes the influences of Nt on $h(\eta)$. As the curvd of $h(\eta)$ shows to rising for larger values of Nt .

VI. Numerical Results

The numerical outcomes of $-\theta'(0)$ for varous values of physical parameters Pr , Nb , γ_1 , Sc and M and rest of parameters are fixed in the Table 1. The significant outcomes of Pr , it is seen that the values of the Pr and $-\theta'(0)$ are found to be same behavior of increasing and $Nb = 0.1$, $\gamma_1 = 0.5$, $Sc = 0.1$ and $M = 0.1$. The values of $-\theta'(0)$ found to be declines as well as Nb is increasing and rest of the physical parameters are fixed like as $Pr = 2.0$, $\gamma_1 = 0.5$, $Sc = 0.1$ and $M = 0.1$. The values of $-\theta'(0)$ found to be declines as well as γ_1 is increasing and rest of the physical parameters are fixed like as $Pr = 2.0$, $Nb = 0.1$, $Sc = 0.1$ and $M = 0.1$. The values of $-\theta'(0)$ found to be declines as well as Sc is increasing and rest of the physical parameters are fixed like as $Pr = 2.0$, $Nb = 0.1$, $\gamma_1 = 0.5$ and $M = 0.1$. The significant outcomes of M , it is seen that the values of the M and $-\theta'(0)$ are found to be same behavior of increasing and $Nb = 0.1$, $\gamma_1 = 0.5$, $Sc = 0.1$ and $Pr = 2.0$.

Table 1: Numerical results of $-\theta'(0)$ for different valuesof physical parameters.

Pr	Nb	γ_1	Sc	M	$-\theta'(0)$
2.0	0.1	0.5	0.1	0.1	0.37418
2.5					0.37859
3.0					0.38081
2.0	0.1				0.37418
	0.2				0.36638
	0.3				0.35847
	0.1	0.5			0.37418
		0.7			0.29654
		0.9			0.07757
		0.5	0.0		0.67019
			0.1		0.37418
			0.2		0.018894
			0.1	0.1	0.37418
				0.5	0.39915
				0.7	0.41206

The numerical outcomes of $-\gamma'(0)$ for various values of physical parameters St , γ_1 , Sc and M and rest of the physical parameters are fixed in the Table 2. The significant outcomes of Sc , it is seen that the values of the Sc and $-\gamma'(0)$ are found to be same behavior of increasing and $\gamma_1 = 0.5$, $St = 1.0$, $M = 0.1$. The significant outcomes of γ_1 , it is seen that the values of the γ_1 and $-\gamma'(0)$ are found to be same behavior of increasing and $Sc = 0.5$, $St = 1.0$, $M = 0.1$. The values of $-\gamma'(0)$ found to be declines as well as M is increasing and rest of the physical parameters are fixed like as $\gamma_1 = 0.5$, $St = 1.0$, $Sc = 1.0$. The values of $-\gamma'(0)$ found to be declines as well as St is increasing and rest of the physical parameters are fixed like as $\gamma_1 = 0.5$, $M = 0.1$, $Sc = 1.0$.

Table 2: Numerical results of $-\gamma'(0)$ for different valuesof physical parameters.

Sc	γ_1	M	St	$-\gamma'(0)$
1.0	0.5	0.1	1.0	1.1630
2.0				1.7597
3.0				2.2518
1.0	0.5			1.1630
	0.7			1.5356
	0.9			2.3569
	0.5	0.1		1.1630
		0.5		1.0138
		0.9		0.92254
		0.1	1	1.1630
			2	1.0749
			3	0.99045

Table 3: Numerical results of $-h'(0)$ for different valuesof physical parameters.

Le	γ_1	Nb	M	$-h'(0)$
1.0	0.5	0.3	0.1	1.1718
2.0				1.7453
3.0				2.1803
1.0	0.5			1.1718
	0.7			1.4405

	0.9			2.0275
	0.5	0.1		1.1084
		0.3		1.1718
		0.5		1.1915
		0.1	0.1	1.1718
			0.5	1.0706
			0.9	1.0083

The numerical outcomes of $-h'(0)$ for various values of physical parameters Le , γ_1 , Nb and M and rest of parameters are fixed in the Table 3. The significant outcomes of Le , it is seen that the values of the Sc and $-h'(0)$ are found to be same behavior of increasing and $\gamma_1 = 0.5$, $Nb = 0.3$, $M = 0.1$. The significant outcomes of γ_1 , it is seen that the values of the γ_1 and $-h'(0)$ are found to be same behavior of increasing $Le = 1.0$, $Nb = 0.3$, $M = 0.1$. The values of $-h'(0)$ found to be increasing as well as Nb is increasing and rest of the physical parameters are fixed like as $= 1.0$, $\gamma_1 = 0.5$, $M = 0.1$. The values of $-h'(0)$ found to be declines as well as M is increasing and rest of the physical parameters are fixed like as $= 1.0$, $Nb = 0.3$, $\gamma_1 = 0.5$.

Table 3: Values of Sharewood Number and Nusselt Number for different values of Pr when rest of the physical parameters are fixed.

Pr	Sharewood Number		Nusselt Number	
	Ref: [36]	Present	Ref: [36]	Present
0.5	0.34689118	0.3468912	1.61983352	1.619336
1.0	0.57428288	0.5742829	1.80285833	1.802859
3.0	1.15942580	1.1594260	2.33075212	2.330753
5.0	1.56331503	1.5633150	2.71619820	2.716199

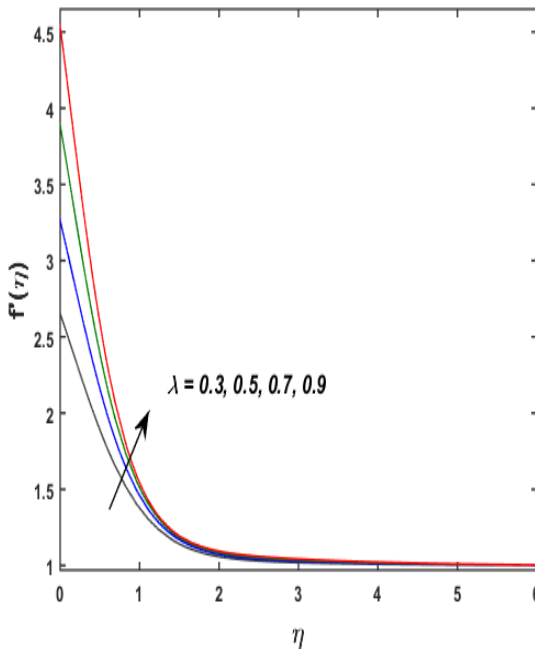


Fig. 1: Variation of λ on $f'(\eta)$.

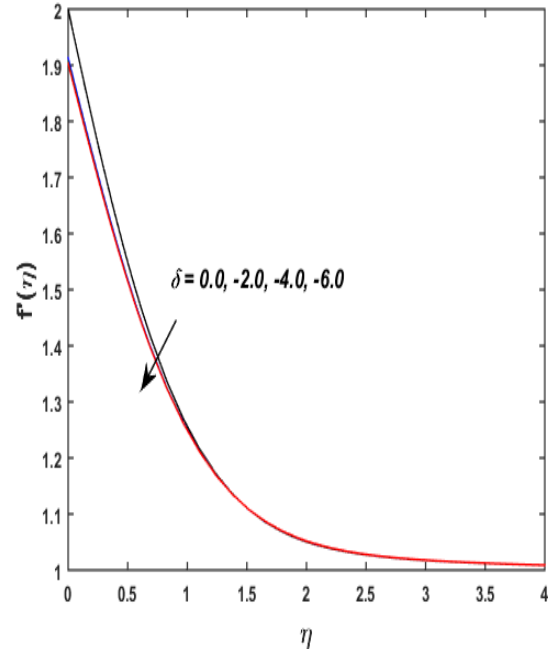


Fig. 2: Variation of δ on $f'(\eta)$.

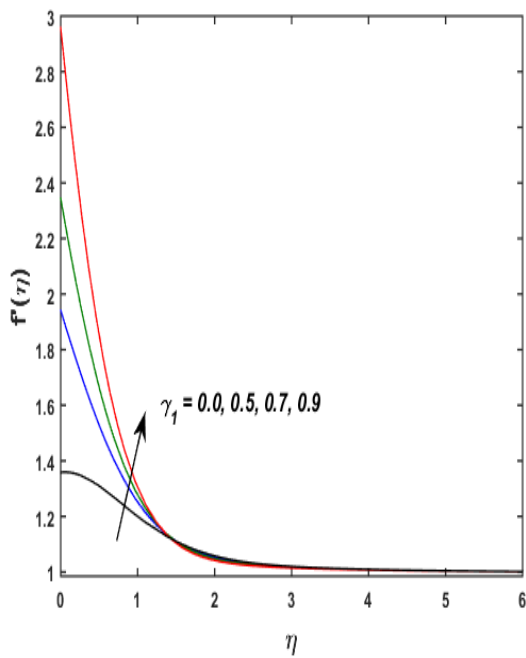


Fig. 3: Variation of γ_1 on $f'(\eta)$.

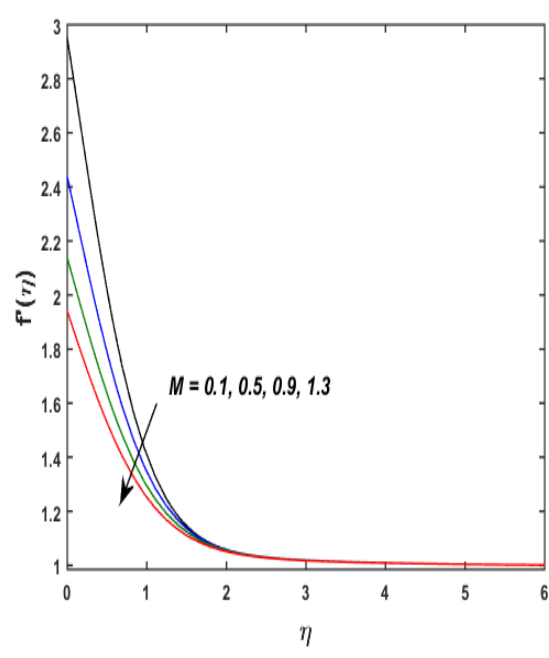


Fig. 4: Variation of M on $f'(\eta)$.

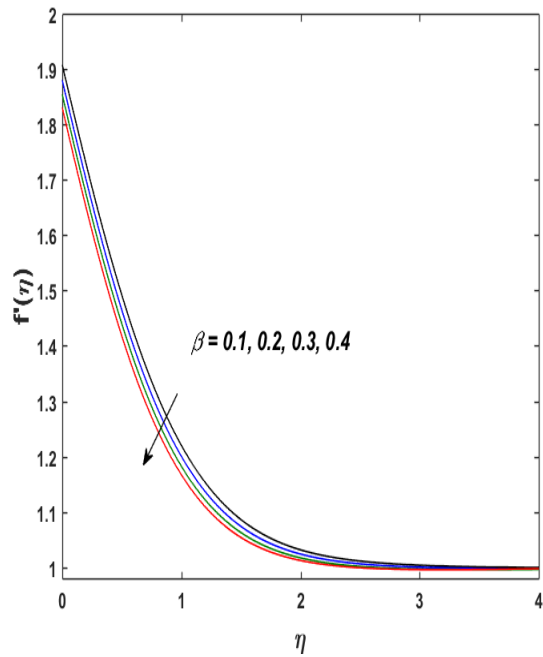


Fig. 5: Variation of β on $f'(\eta)$.

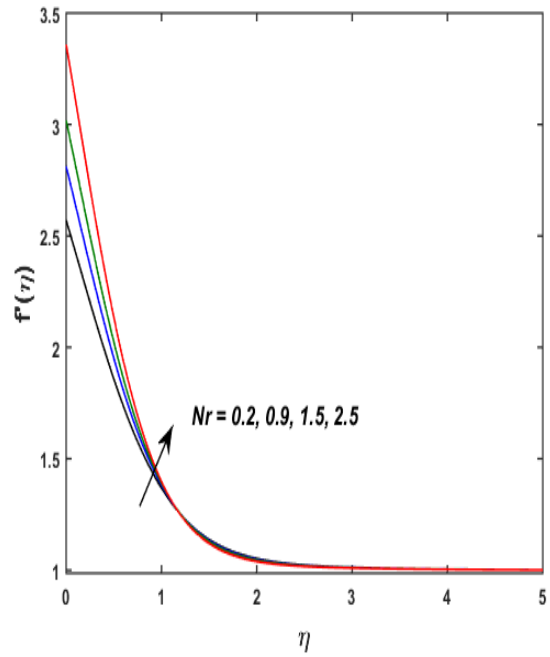


Fig. 6: Variation of Nr on $f'(\eta)$.

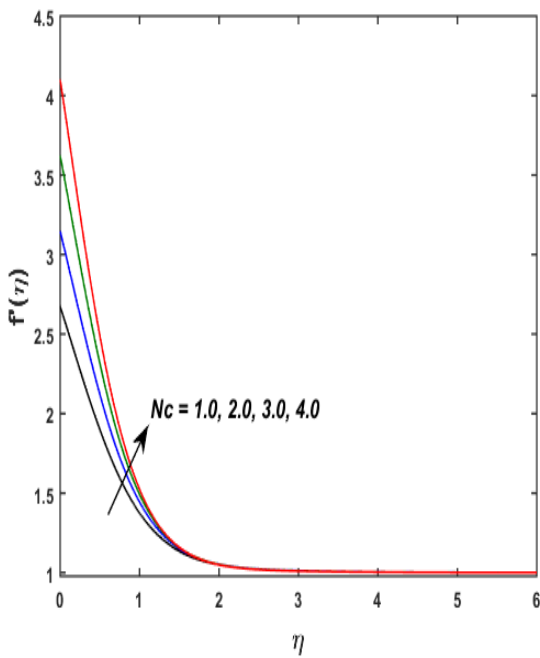


Fig. 7: Variation of Nc on $f'(\eta)$.

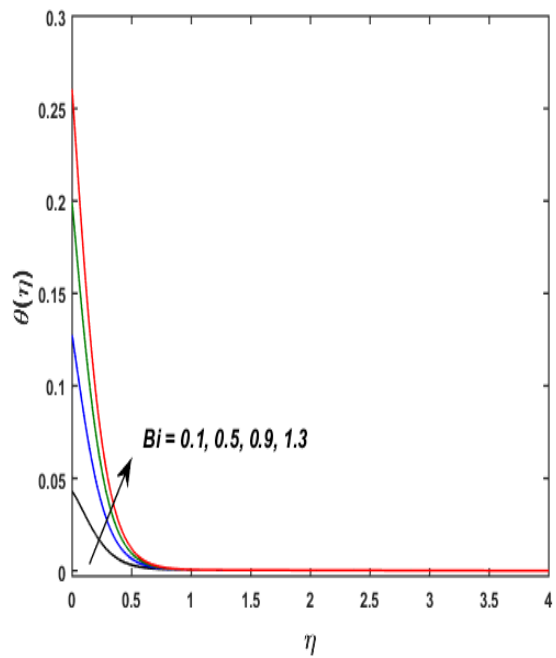


Fig. 8: Variation of Bi on $\theta(\eta)$.

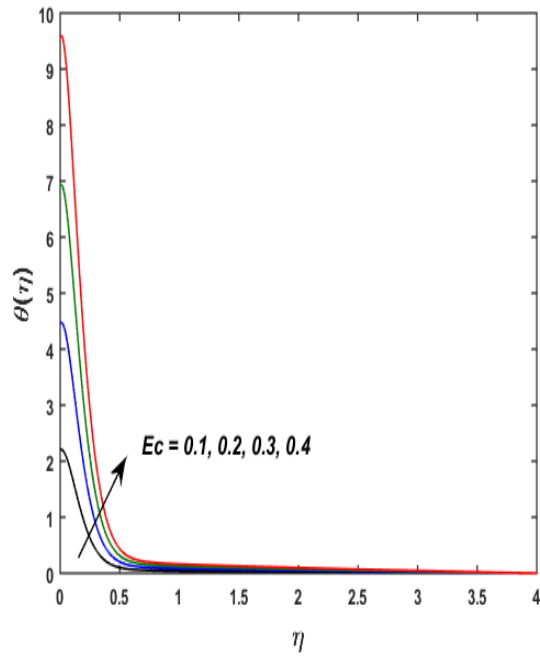


Fig. 9: Variation of Ec on $\theta(\eta)$.

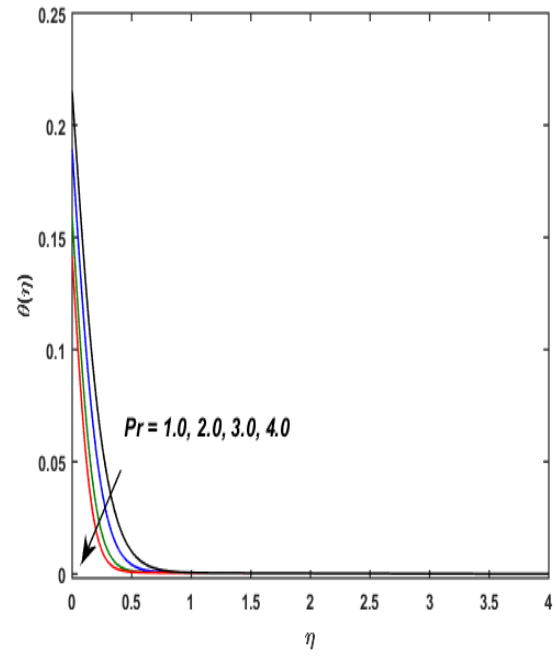


Fig. 10: Variation of Pr on $\theta(\eta)$.

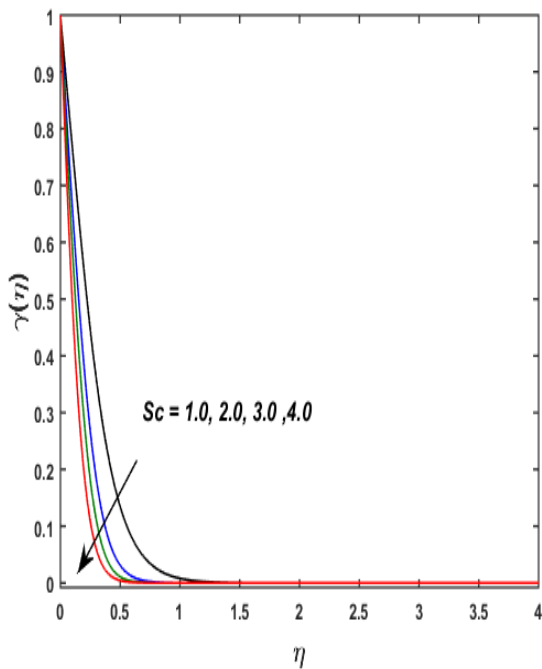


Fig. 11: Variation of Sc on $\gamma(\eta)$.

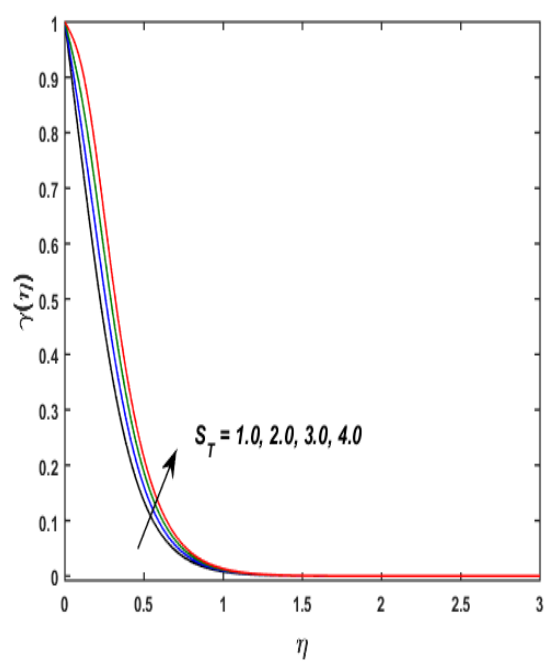


Fig. 12: Variation of S_T on $\gamma(\eta)$.

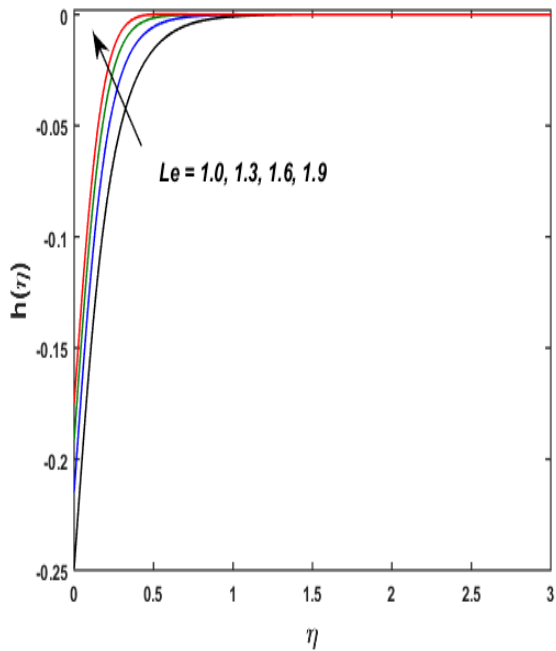


Fig. 13: Variation of Le on $h(\eta)$.

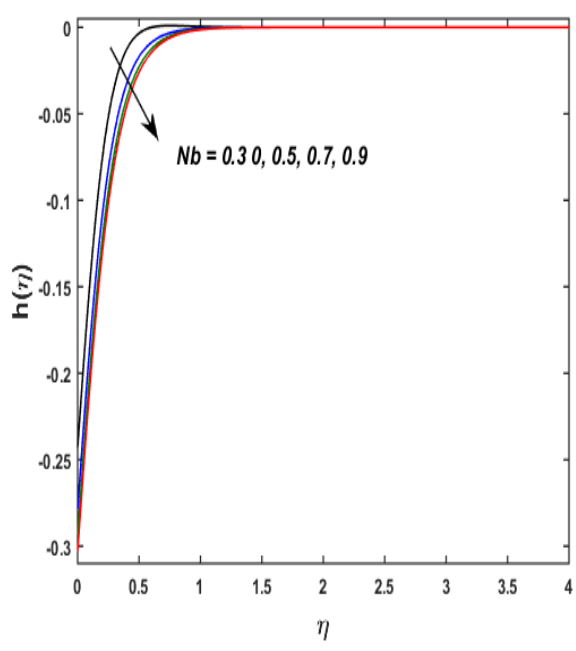


Fig. 14: Variation of Nb on $h(\eta)$.

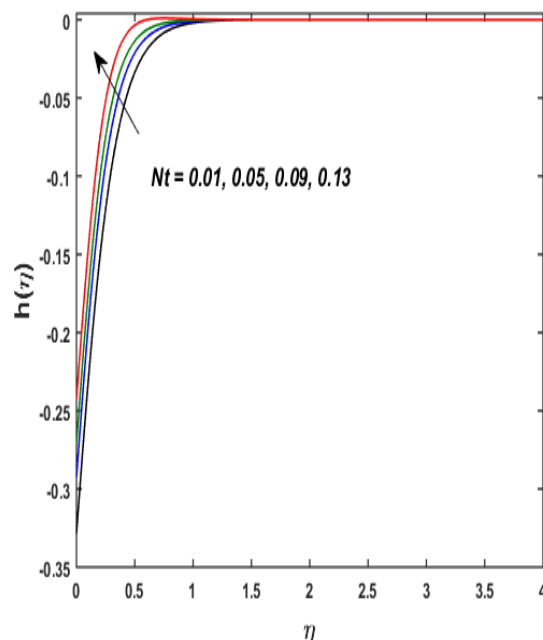


Fig. 15: Variation of Nt on $h(\eta)$.

VII. Final remarks

Nanomaterials Maxwell fluid flow over an exponentially stretching surface is deliberated in the presentscrutiny. Second grade slip and chemical reactions effects with Viscous dissipation in the presence of Buongiorno's model are highlighted. The main acheivemnet of the our studyis presented below:

- The velocity profile enhances due to enhancing the values of λ while velicity profile declines as rises the values of δ .
- The velocity profile declines as well as the values of the β rises and the values of the velocity profile $f'(\eta)$ ehnaces due to enhances the values of Nr .
- The values of Nusselt number found to be declines when the values of Nb is increasing.
- The values of Sc and $\gamma(\eta)$ enhances as wellas declines the curves of $\gamma(\eta)$ but opposite behavior of S_T and (η) for both increasing.
- In Table 3, our results are found to be good agreement with decay results.

References

- [1]. Maxwell, J. C. (1867). Iv. on the dynamical theory of gases. *Philosophical transactions of the Royal Society of London*, (157), 49-88.
- [2]. Sadeghy, K., Najafi, A. H., & Saffaripour, M. (2005). Sakiadis flow of an upper-conveeted Maxwell fluid. *International Journal of Non-Linear Mechanics*, 40(9), 1220-1228.
- [3]. Mukhopadhyay, S., De, P. R., & Layek, G. C. (2013). Heat transfer characteristics for the Maxwell fluid flow past an unsteady stretching permeable surface embedded in a porous medium with thermal radiation. *Journal of Applied Mechanics and Technical Physics*, 54(3), 385-396.
- [4]. Xu, H., Fan, T., & Pop, I. (2013). Analysis of mixed convection flow of a nanofluid in a vertical channel with the Buongiorno mathematical model. *International Communications in Heat and Mass Transfer*, 44, 15-22.
- [5]. Nadeem, S., Haq, R. U., & Khan, Z. H. (2014). Numerical study of MHD boundary layer flow of a Maxwell fluid past a stretching sheet in the presence of nanoparticles. *Journal of the Taiwan Institute of Chemical Engineers*, 45(1), 121-126.
- [6]. Khan, M., Malik, R., Munir, A., & Khan, W. A. (2015). Flow and heat transfer to Sisko nanofluid over a nonlinear stretching sheet. *PLoS One*, 10(5), e0125683.
- [7]. Khan, W. A., Khan, M., Alshomrani, A. S., & Ahmad, L. (2016). Numerical investigation of generalized Fourier's and Fick's laws for Sisko fluid flow. *Journal of Molecular Liquids*, 224, 1016-1021.
- [8]. Shafique, Z., Mustafa, M., & Mushtaq, A. (2016). Boundary layer flow of Maxwell fluid in rotating frame with binary chemical reaction and activation energy. *Results in physics*, 6, 627-633.
- [9]. Hsiao, K. L. (2017). Combined electrical MHD heat transfer thermal extrusion system using Maxwell fluid with radiative and viscous dissipation effects. *Applied Thermal Engineering*, 112, 1281-1288.
- [10]. Khan, W. A., Irfan, M., & Khan, M. (2017). An improved heat conduction and mass diffusion models for rotating flow of an Oldroyd-B fluid. *Results in physics*, 7, 3583-3589.
- [11]. Aman, S., Al-Mdallal, Q., & Khan, I. (2018). Heat transfer and second order slip effect on MHD flow of fractional Maxwell fluid in a porous medium. *Journal of King Saud University-Science*.
- [12]. Nazeer, M., Ali, N., Javed, T., & Razzaq, M. (2019). Finite element simulations for energy transfer in a lid-driven porous square container filled with micropolar fluid: impact of thermal boundary conditions and Peclet number. *International Journal of Hydrogen Energy*, 44(14), 7656-7666.

- [13]. Abbas, S. Z., Khan, W. A., Kadry, S., Khan, M. I., Waqas, M., & Khan, M. I. (2020). Entropy optimized Darcy-Forchheimernanofluid (silicon dioxide, molybdenum disulfide) subject to temperature dependent viscosity. *Computer methods and programs in biomedicine*, 190, 105363.
- [14]. Nazeer, M., Hussain, F., Ahmad, M. O., Saeed, S., Khan, M. I., Kadry, S., & Chu, Y. M. (2020). Multi-phase flow of Jeffrey Fluid bounded within magnetized horizontal surface. *Surfaces and Interfaces*, 22, 100846.
- [15]. Nazeer, M., Hussain, F., Shahzad, Q., Khan, M. I., Kadry, S., & Chu, Y. M. (2020). Perturbation solution of the multiphase flows of third grade dispersions suspended with Hafnium and crystal particles. *Surfaces and Interfaces*, 22, 100803.
- [16]. Rubbab, Q., Nazeer, M., Ahmad, F., Chu, Y. M., Khan, M. I., & Kadry, S. (2020). Numerical simulation of advection-diffusion equation with caputo-fabrizio time fractional derivative in cylindrical domains: Applications of pseudo-spectral collocation method. *Alexandria Engineering Journal*, 60(1), 1731-1738.
- [17]. Chu, Y. M., Nazeer, M., Khan, M. I., Ali, W., Zafar, Z., Kadry, S., & Abdelmalek, Z. (2020). Entropy analysis in the Rabinowitsch fluid model through inclined Wavy Channel: Constant and variable properties. *International Communications in Heat and Mass Transfer*, 119, 104980.
- [18]. Nazeer, M., Ali, N., Ahmad, F., Ali, W., Saleem, A., Ali, Z., & Sarfraz, A. (2020). Effects of radiative heat flux and joule heating on electro-osmotically flow of non-Newtonian fluid: Analytical approach. *International Communications in Heat and Mass Transfer*, 117, 104744.
- [19]. Choi, S. U., & Eastman, J. A. (1995). *Enhancing thermal conductivity of fluids with nanoparticles* (No. ANL/MSD/CP-84938; CONF-951135-29). Argonne National Lab., IL (United States).
- [20]. Lee, J. H., Hwang, K. S., Jang, S. P., Lee, B. H., Kim, J. H., Choi, S. U., & Choi, C. J. (2008). Effective viscosities and thermal conductivities of aqueous nanofluids containing low volume concentrations of Al₂O₃ nanoparticles. *International Journal of Heat and Mass Transfer*, 51(11-12), 2651-2656.
- [21]. Buongiorno, J. (2006). Convective transport in nanofluids. *Journal of heat transfer*, 128(3), 240-250.
- [22]. Öztop, H.F.; Abu-Nada, E. Numerical study of natural convection in partially heated rectangular enclosures filled with nanofluids. *Int. J. Heat Fluid Flow* 2008, 29, 1326–1336.
- [23]. Santra, A.K.; Sen, S.; Chakraborty, N. Study of heat transfer due to laminar flow of copper–water nanofluid through two isothermally heated parallel plates. *Int. J. Therm. Sci.* 2009, 48, 391–400.
- [24]. Nadeem, S., Malik, M. Y., & Abbas, N. (2019). Heat transfer of three dimensional micropolar fluids on Riga plate. *Canadian Journal of Physics*, (ja).
- [25]. Nadeem, S., & Abbas, N. (2019). Effects of MHD on Modified Nanofluid Model with Variable Viscosity in a Porous Medium. In *Nanofluid Flow in Porous Media*. IntechOpen.
- [26]. Alblawi, A., Malik, M. Y., Nadeem, S., & Abbas, N. (2019). Buongiorno's Nanofluid Model over a Curved Exponentially Stretching Surface. *Processes*, 7(10), 665.
- [27]. Awan, A. U., Rehman, H. U., Tahir, M., & Ramzan, M. (2021). Optical soliton solutions for resonant Schrödinger equation with anti-cubic nonlinearity. *Optik*, 227, 165496.
- [28]. Ozair, M., Hussain, T., Awan, A. U., Aslam, A., Khan, R. A., Ali, F., & Tasneem, F. (2020). Bio-inspired Analytical Heuristics to Study Pine Wilt Disease Model. *Scientific reports*, 10(1), 1-15.
- [29]. Awan, A. U., Abid, S., & Abbas, N. (2020). Theoretical study of unsteady oblique stagnation point based Jeffrey nanofluid flow over an oscillatory stretching sheet. *Advances in Mechanical Engineering*, 12(11), 1687814020971881.
- [30]. Shah, N. A., Awan, A. U., Khan, R., Tili, I., Farooq, M. U., & Salah, B. (2020). Free convection Hartmann flow of a viscous fluid with damped thermal transport through cylindrical tube. *Chinese Journal of Physics*.
- [31]. Awan, A. U., Abid, S., Ullah, N., & Nadeem, S. (2020). Magnetohydrodynamic oblique stagnation point flow of second grade fluid over an oscillatory stretching surface. *Results in Physics*, 18, 103233.
- [32]. Firdous, H., Husnine, S. M., Hussain, F., & Nazeer, M. (2020). Velocity and thermal slip effects on two-phase flow of MHD Jeffrey fluid with the suspension of tiny metallic particles. *Physica Scripta*, 96(2), 025803.
- [33]. Nadeem, S., Abbas, N., & Malik, M. Y. (2020). Inspection of hybrid based nanofluid flow over a curved surface. *Computer methods and programs in biomedicine*, 189, 105193.
- [34]. Nadeem, S., Amin, A., & Abbas, N. (2020). On the stagnation point flow of nanomaterial with base viscoelastic micropolar fluid over a stretching surface. *Alexandria Engineering Journal*, 59(3), 1751-1760.
- [35]. Abbas, N., Nadeem, S., & Saleem, A. (2020). Computational analysis of water based Cu-Al 2 O 3/H 2 O flow over a vertical wedge. *Advances in Mechanical Engineering*, 12(11), 1687814020968322.
- [36]. Chakraborty, T., Das, K., & Kundu, P. K. (2018). Framing the impact of external magnetic field on bioconvection of a nanofluid flow containing gyrotactic microorganisms with convective boundary conditions. *Alexandria engineering journal*, 57(1), 61-71.

M. N. Khan, et. al. "Transportation of nanomaterial Maxwell fluid flow with chemical reaction under the second orderslips effect: Nonlinear stretching." *The International Journal of Engineering and Science (IIES)*, 11(9), (2022): pp. 19-29.